scientific reports

Check for updates

OPEN

Energy dispersive X-ray fluorescence characterization of soil and its geological provenance assessment – Mvengue subdivision of Cameroon

Bonaventure Mvogo Aloa[1], Jean Félix Beyala Ateba[1,2]✉, Cebastien Joel Guembou Shouop[2], Jean Marie Ema'a Ema'a[3], Jean Faustin Sabouang[2], Dieu-Souffit Gondji[1,4] & Germain Hubert Ben-Bolie[1]

This study aimed to perform the elemental characterization of soil samples for heavy metal pollution and geological provenance close to the uranium deposit. The investigated area is located in two localities, Awanda and Mvengue, in the Mvengue Subdivision, Ocean Division, South Region of Cameroon. The elemental composition of soil samples was determined using an XEPOS EDXRF (Energy Dispersion X-ray Fluorescence) spectrometer. The Spectro XRF Analyzer Pro software interface was used for spectral acquisition and quantification. Soil elemental characterization and differentiation revealed the mass fractions of major, minor, and trace elements. SiO_2 (49.81%) and Al_2O_3 (42.18%) were the predominant elements in all the soil samples investigated. The correlation between K_2O and Al_2O_3 illustrates that the mass fraction of K-bearing minerals has a notable impact on the distribution of Al. Herron's classification of the analyzed soil samples displayed two different categories. Shale represented 70% of the analyzed materials, and Arkose made up the remaining 30%. By comparing the results with the well-established diagram for tectonic discrimination of geological provenance, the origin of the studied samples was determined to comprehend ongoing processes within the study area. It was apparent that all examined soil samples represented residual material from the passive margin. The findings of this study suggested that the examined and surrounding regions were shaped by erosion and weathering processes rather than tectonic activity.

Keywords EDXRF, Geological provenance, Elemental composition, Major element, Trace element, Herron's diagram, Tectonic discrimination

The Earth's surface is covered by a thin layer of material known as soil, which is formed by the weathering of rocks. Geochemical analysis of soil can provide valuable insights, as immobile oxide major and trace elements have been identified as useful indicators of land sources, weathering, tectonic settings, and environmental evolution[1–3].

The southern region of Cameroon, which is situated in the Gulf of Guinea, presents promising prospects for mineralogical and geological surveys. Exploration works carried out in this area by the French Office of Geological and Mining Research[4] confirmed the existence of uranium-bearing formations in Lolodorf. Moreover, many investigations have defined the area as a high background radiation area (HBRA)[4–7]. Therefore, attention should mainly focus on environmental monitoring in these areas[8]. Several studies have been conducted to evaluate natural radioactivity in the uranium-bearing areas of Lolodorf and its surroundings[4–7,9,10]. There is limited information available on the area's geochemical background. It is therefore essential to analyze the elemental composition of environmental samples, including soil, water, plants, and air, to obtain geochemical baseline

[1]Laboratory of Atomic, Molecular and Nuclear Physics, Department of Physics, Faculty of Science, University of Yaoundé I, P.O. Box: 812, Yaoundé, Cameroon. [2]Radiological Safety and Nuclear Security Authority, P O Box 33732, Yaoundé, Cameroon. [3]Department of Physics, Bertoua Higher Teacher's Training College, University of Bertoua, P.O. Box: 55, Bertoua, Cameroon. [4]Research Centre for Nuclear Science and Technology, Institute of Geological and Mining Research, P.O. Box 4110, Yaoundé, Cameroon. ✉email: bajeanfelix@yahoo.fr

data, which is a crucial component of strategic and systematic geoscience surveys[11,12]. This approach will aid in identifying any potential mass fraction enhancement of harmful elements in the area. The data collected will help to understand the environmental history of the area and will assist in identifying the geological provenance of the area under investigation.

To achieve this goal, energy-dispersive X-ray fluorescence (EDXRF) spectroscopy was used to characterize the environmental samples. Compared with the use of alpha particles, and other types of spectroscopy methods, such as atomic absorption spectrometry (AAS), inductively coupled plasma-atomic emission spectrometry (ICP–AES), and inductively coupled plasma–mass spectrometry (ICP-MS) which require delicate preparation and alteration of the sample during preparation, it is widely used as a non-destructive and relatively rapid technique[13–16]. EDXRF is a valuable analytical technique widely used in the fields of geochemistry and mineralogy to determine the elemental composition of rocks, minerals, and other geological materials and to assess the geological provenance of samples[17–21]. More recently, geochemical data from terrestrial deposits have been used as a provenance tool by researchers. In 2023, Carita et al. (2023) demonstrated that both K_2O/Na_2O and immobile trace-elements ratio are suitable indicators of geological deposits' provenance[22]. Moreover, high-resolution XRF (X-ray fluorescence) core scanning could be used to reveal the depositional history of geological formations, as recently assessed by Shane et al. (2024)[23] for the case of northeastern British Columbia in Canada. In Cameroon, a few studies have been performed on elemental composition and geological provenance of geological (sand) samples from Douala using the XRF method. Guembou et al. (2019) research showed that XRF yielded quantitative major, minor, and trace element mass fractions used in tectonic discrimination diagrams. They found that the investigated area was deposited in a passive margin environment[19,20].

This study aims to perform a quantitative elemental analysis of soil samples collected around the high background radiation area (HBRA) in Lolodorf. The elemental mass fractions of oxide and minor elements are used thereafter to determine the geological origin of the investigated soil. Two locations surrounding the uranium deposit in Lolodorf (Awanda and Mvengue) yielded a total of ten soil samples. The analyzed soil samples were investigated using an energy dispersive X-ray fluorescence spectrometer (SPECTRO XEPOS) to obtain more sensitive and accurate results. This method has recently been used in Cameroon for accurate elemental characterization of samples and determination of the geological provenance of a certain type of soil[17–21,24–26]. While this study focuses on assessing the geological provenance of the soil through oxide geochemistry, understanding these characteristics is also relevant for evaluating soil behavior in agro-environmental settings near uranium-rich formations.

Materials and methods

Description of the study areas

The study area is located in the southern region of Cameroon in the Mvengue Subdivision, Ocean Division, close to the Lolodorf uranium deposit (see Fig. 1). Two sampling sites, Awanda and Mvengue, were chosen for their proximity to the uranium deposits. The rural district of Mvengue and the village of Awanda have populations of approximately 1326 and 936 inhabitants, respectively. The population density ranges from 8 to 11 individuals per km^2. Over 80% of the population primarily engages in subsistence agriculture[27].

The study area is located in an equatorial climate characterized by two rainy seasons and two dry seasons. The dry seasons are from December to February and from July to August, while the rainy seasons extend from September to November and from March to June. The annual rainfall ranges from 1500 to 2000 mm, with 70–80% relative humidity recorded throughout the year. The mean temperature of the zone varies from 25 to 26 °C. According to the world map of the Köppen-Geiger climate classification[28]this climate is classified as Am.

The investigated area belongs to the Nyong complex, with formations mainly composed of paleoprotozoic edges[29]. There are two types of soil: ferralitic soils with deep-red and yellow–red colors and hydromorphic soils found in the southern region of Cameroon. These soils are globally acidic. The lithology in this region typically consists of syenites and radioactive source rocks, composed of syntectonic syenites that appear to be associated with a shear zone[10].

Soil sampling and sample preparation

Ten soil samples were collected from Awanda and Mvengue, two areas close to Lolodorf's uranium deposits, in the southern region of Cameroon, as depicted in Fig. 1. The sampling points are located in agricultural zones. To guarantee representativeness and prevent contamination, appropriate on-site sampling techniques were employed during the collection of all samples[9]. At each sampling point, an area of 1 m^2 was identified. The humus layer was removed with a flat-bladed shovel to remove new soil formed as a result of weathering and erosion processes. Soil samples were taken at depths between 5 and 15 cm from each corner of the 1 m^2 area and the center, ensuring that metric measurements and units were strictly adhered to. This method ensured that samples were collected to represent the natural soil matrix for provenance analysis, without targeting anthropogenic influence or agricultural amendment. The five subsamples of soil were pooled together to form a composite sample. A labeled polyethylene bag was used to store approximately 2 kg of each fresh sample. The geographic coordinates of sampling points and soil sample codes are given in Table 1. The soil samples collected were transported to the Institute of Geological and Mining Research in Yaoundé for proper preparation.

In the laboratory, every soil sample was prepared according to the Nuclear Technology Section of IRGM protocols as per[30]. Any large particles were removed from the samples, and the remaining particles were dried in a Gallenkamp Hotbox oven with a fan size of 2 m^3 for 3 days at 100 °C. The samples were then ground using a Frisch Pulverizette from Germany at speeds up to 60 rpm and sieved at approximately 2 mm diameter. To ensure greater accuracy in the XRF analysis, 10 g of each sieved sample was crushed in an agate mortar to obtain diameters in the micron range (~2 µm).

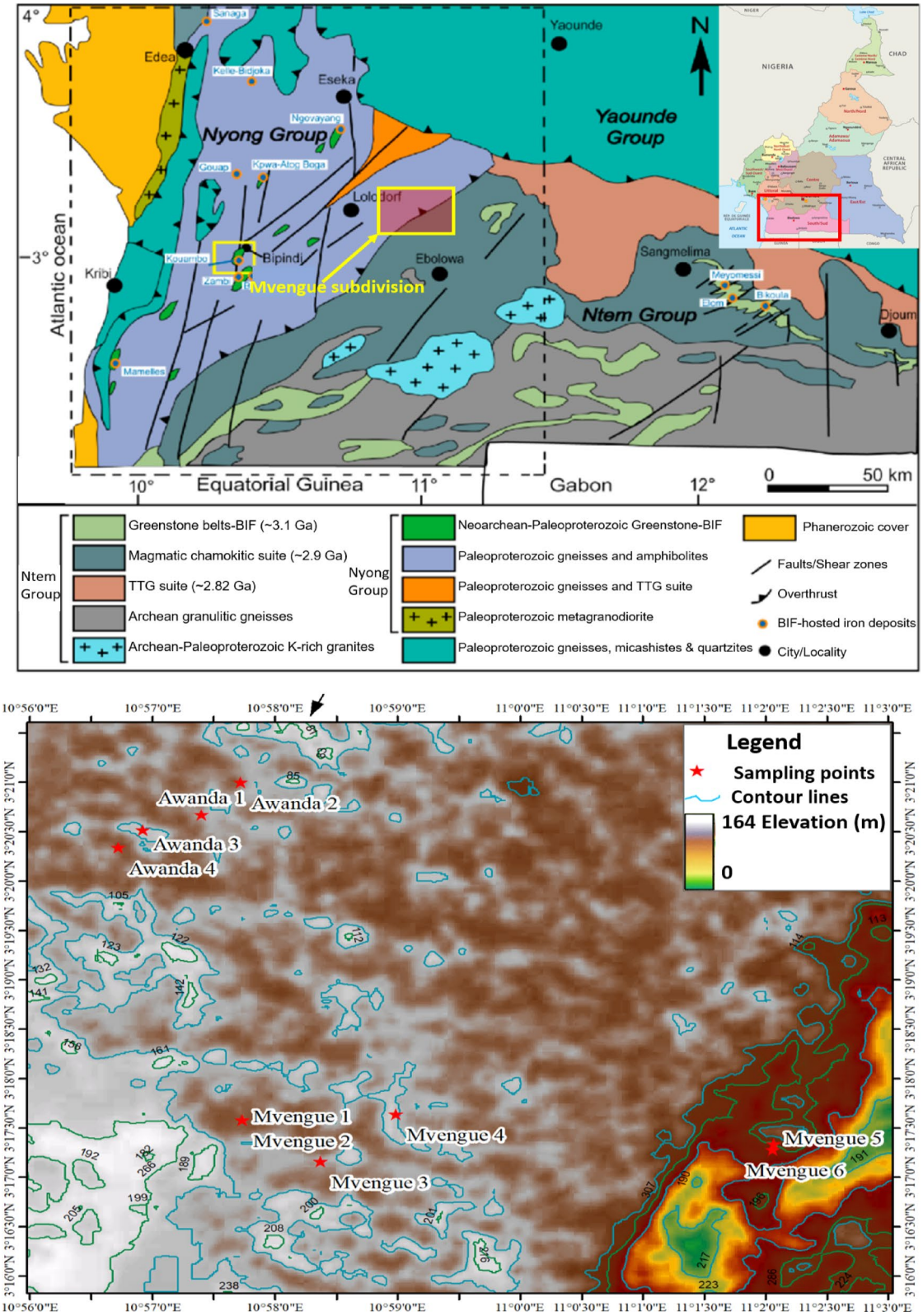

Fig. 1. Map of the Awanda and Mvengue study areas, located in the Mvengue Subdivision, Ocean Division, close to the Lolodorf uranium deposit in the southern region of Cameroon[31].

Sampling points	Codes	Latitude	Longitude
Awanda 1	A1	3. 344,592° N	10.956716° E
Awanda 2	A2	3.350253° N	10.962013° E
Awanda 3	A3	3.342444° N	10.948691° E
Awanda 4	A4	3.338782° N	10.945372° E
Mvengue 1	M1	3.292915° N	10.962242° E
Mvengue 2	M2	3.292915° N	10.962242° E
Mvengue 3	M3	3.285654° N	10.972852° E
Mvengue 4	M4	3.293807° N	10.983126° E
Mvengue 5	M5	3.288770° N	11.034485° E
Mvengue 6	M6	3.287544° N	11.034338° E

Table 1. Geographic coordinates of sampling points and soil sample codes.

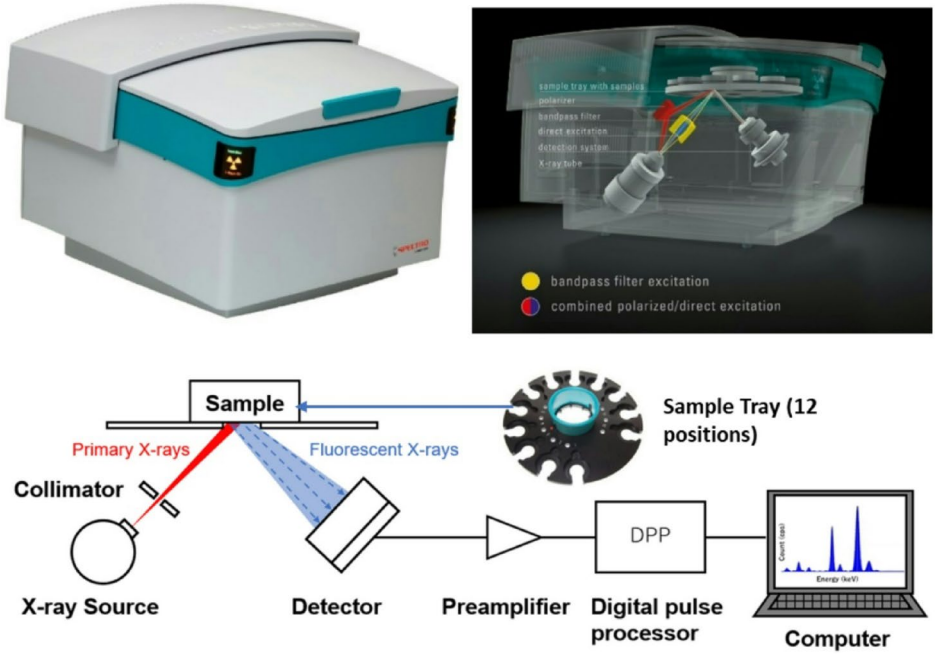

Fig. 2. Experimental setup. Up left: Picture of the Spectro XEPOS EDXRF equipment. Up right: Schematic picture of the operating principle of the equipment. Bottom: Schematic diagram of the basic operating principle of the EDXRF Spectro XEPOS spectrometer.

XRF spectrometry equipment and analysis

The elemental composition of the soil samples was determined using an energy dispersive X-ray fluorescence (EDXRF) Spectro Xepos spectrometer (XPOS05) at the National Radiation Protection Agency (in the laboratory of radioanalysis and spectrometry) in Yaounde, Cameroon. The Spectro EDXRF Analyzer Pro software interface was used for spectral acquisition and quantification. Mass fraction calculations of major, minor, and trace elements in the soil samples were conducted using TurboQuant II, a powerful tool for effortless analysis of unknown samples. This method uses automatic matrix correction without requiring specific calibration for every change in the matrix. A simplified schematic diagram of the equipment is presented in Fig. 2, along with a picture of the EDXRF Spectro Xepos Spectrometer. The spectrometer is fitted with a 30 mm^2 Si-drift detector (SDD) equipped with a Peltier cooling system to attain high spectral resolution (FWHM ≤ 155 eV for Mn-Kα), ultra-sensitivity, precision, a high-count rate (up to 1000000 cps), and low detection limits (to 1 ppm or lower). The detailed detector characteristics and measuring conditions are shown in Table 2.

To ensure accurate and precise investigation of the soil data, in accordance with quality control protocols, we used Certified Reference Materials (CRMs) from the Wageningen Evaluating Programs for Analytical Laboratories (WEPAL), namely, Organic Ferrasol (ISE998) and Heavy Clay (ISE953). The obtained results, as displayed in Table 3, show excellent agreement between measured and certified values. An exception is observed for MgO with little effect, as the deviation was found around 20%.

Uncertainty calculations were performed for the EDXRF measurements. The relative uncertainty of the analyzed soil sample is given by the following equation:

Measurements			Measurement details							
	Voltage (kV)	Current (mA)	Plate correction factor	Number of channels	Resolution FWHM (Mn-K_α) (eV)	Input count rate cps	Lifetime (S)	Relative dead time (%)	Zero peak rate (cps)	Temperature of the detector (℃)
E ≤ 3 keV	22.6	1.781	1,000,000	4096	133.1	38,614	137	9	2,000,000	-30
3 keV ≤ E ≤ 6 keV	22.6	1.781	1,000,000	4096	133.8	488,452	85	43.2	2,000,000	-30
6 keV ≤ E ≤ 19 keV	45.2	0.889	1,000,000	4096	133.8	219,142	98	34.4	2,000,000	-30
E > 19 keV	50.2	0.799	1,000,000	4096	133.8	7634	125	16.5	2,000,000	-30

Table 2. Measurement conditions for the EDXRF analysis of soil samples using the spectro Xepos spectrometer. The atmosphere is always air, the duration of each measurement is set to 150 s, and the anode material is made of Pd/Co.

ISE953	Certified values	Measured values	Deviation*	ISE998	Certified values	Measured values	Deviation
Al_2O_3 (%)	24.79	24.10	2.78%	Al_2O_3 (%)	25.40	24.83	2.24%
SiO_2 (%)	63.33	63.77	0.69%	SiO_2 (%)	64.29	65.96	2.60%
K_2O (%)	7.71	7.77	0.74%	K_2O (%)	4.23	4.12	2.60%
CaO (%)	1.45	1.51	4.22%	CaO (%)	0.58	0.57	1.48%
Ti	2742	2865	4.49%	Ti	3758	3681	2.05%
				P_2O_5 (%)	0.13	0.14	5.43%
MnO	1014	1067	5.23%	MnO	178.60	183.30	2.63%
Fe_2O_3 (%)	6.69	6.81	1.85%	Fe_2O_3 (%)	6.57	6.02	8.40%

Table 3. Measurement results (in mg/kg) of certified reference materials ISE953 and ISE998. * Deviation values were calculated as the relative error between the measured values over certified values.

$$U(A)/A = k\sqrt{(u(I)/I)^2 + (u(m)/m)^2} \quad (1)$$

For the present work, we considered an enlargement factor k = 1; $u(I)/I$ is the uncertainty linked to the counting statistic and given by the analysis report; I is the count rate of analyzed soil samples; $u(I)$ is the absolute uncertainty of the count rate; and $u(m)/m$ is the uncertainty in the measurement of soil sample masses. Given that the uncertainty in the measurement of soil sample masses follows a rectangular distribution, the uncertainty in the measurement of soil sample masses can be expressed as:

$$u(m)/m = m_{min}/2\sqrt{3}m \quad (2)$$

where m_{min} is the minimum mass detectable by the balance and given by the manufacturer, and m is the measured soil sample mass. We note that the other sources of uncertainty are negligible.

Geological provenance assessment

To track the origin of geological materials, such as soil samples, the geochemical composition, particularly the distribution of major oxides and selected trace elements, is often used. Among these, TiO_2 (or Ti) is widely regarded as one of the most robust and immobile indicators due to its resistance to chemical weathering and its strong lithological association with heavy accessory minerals such as rutile and ilmenite. Consequently, in the present study, TiO_2 was employed as a key discriminator in the application of tectonic setting diagrams, specifically for classifying sedimentary provenance in relation to passive or active margin contexts. Additionally, SiO_2 and Al_2O_3 were considered, as they are frequently used in sedimentary and soil provenance analyses due to their abundance and diagnostic value in reflecting source rock composition and weathering processes. However, their concentrations can be significantly influenced by textural parameters, namely grain size, sorting, and clay content, making them potentially misleading when used in isolation. To account for this, these oxides were interpreted in conjunction with other major oxides to minimize misclassification related to sediment maturity or sedimentary sorting effects[22].

Furthermore, other oxides like CaO, MnO, Fe_2O_3, and MgO were included in the analysis, not only to provide a complete geochemical fingerprint but also because they may contribute to certain geochemical discrimination indices. While their provenance potential is more limited due to higher mobility under certain environmental conditions, such as acidic pH, redox fluctuations, they still offer valuable contextual information, particularly when interpreting the degree of weathering, diagenesis, or secondary enrichment. These parameters collectively inform the geochemical classification and provenance interpretations discussed in the following Sect[22].

Site	Code	SiO_2	TiO_2	Al_2O_3	Fe_2O_3	MnO	CaO	K_2O	P_2O_5	SO_3
MVENGUE	M1	49.27 ± 0.05	1.355 ± 0.001	42.75 ± 0.08	0.956 ± 0.004	0.0400 ± 0.0001	0.0465 ± 0.0003	0.4578 ± 0.0007	0.107 ± 0.001	0.007 ± 0.001
	M2	49.66 ± 0.01	1.266 ± 0.001	41.31 ± 0.05	0.0011 ± 0	0.0325 ± 0.0001	0.068 ± 0.050	0.5463 ± 0.0003	0.106 ± 0.0001	ND
	M3	44.32 ± 0.05	1.183 ± 0.001	46.32 ± 0.09	0.001 ± 0	0.0397 ± 0.0001	0.4349 ± 0.0006	0.7647 ± 0.0009	0.326 ± 0.003	0.064 ± 0.001
	M4	53.89 ± 0.01	1.607 ± 0.001	39.79 ± 0.05	0.736 ± 0.004	0.0285 ± 0.0001	0.084 ± 0.050	0.8478 ± 0.0003	0.116 ± 0.0001	ND
	M5	51.01 ± 0.05	1.452 ± 0.000	40.80 ± 0.08	0.931 ± 0.004	0.0715 ± 0.0001	0.5666 ± 0.0006	0.3586 ± 0.0006	0.305 ± 0.003	ND
	M6	50.84 ± 0.05	1.478 ± 0.001	41.49 ± 0.08	0.920 ± 0.004	0.0259 ± 0.0001	0.0991 ± 0.0003	0.3690 ± 0.0006	0.129 ± 0.002	0.016 ± 0.00
AWANDA	A1	45.56 ± 0.05	1.218 ± 0.001	43.13 ± 0.09	0.0013 ± 0	0.0405 ± 0.0001	0.3917 ± 0.0006	0.5083 ± 0.0008	0.143 ± 0.002	0.019 ± 0.001
	A2	49.78 ± 0.05	1.379 ± 0.001	42.78 ± 0.08	0.914 ± 0.08	0.0257 ± 0.0001	0.0478 ± 0.0002	0.2988 ± 0.0006	0.088 ± 0.001	ND
	A3	51.38 ± 0.05	1.196 ± 0.001	43.37 ± 0.08	0.696 ± 0.003	0.0144 ± 0.0001	0.0207 ± 0.0002	0.4864 ± 0.0007	0.042 ± 0.001	ND
	A4	52.43 ± 0.05	1.462 ± 0.001	40.06 ± 0.08	0.842 ± 0.004	0.0596 ± 0.0001	0.4465 ± 0.0006	0.6361 ± 0.0008	0.350 ± 0.003	ND
MIN		44.32	1.183	39.79	0.001	0.0144	0.02066	0.299	0.042	0.007
MAX		53.89	1.607	46.32	0.956	0.0715	0.5666	0.848	0.350	0.064
Average		49.814	1.360	42.18	0.856	0.038	0.221	0.527	0.171	0.010
Upper crust*		66.6	0.64	15	5.04	0.10	3.59	2.8	0.15	ND

Table 4. Mass fractions (%) of major and minor elements in the investigated soil samples. Upper crust*= [35].

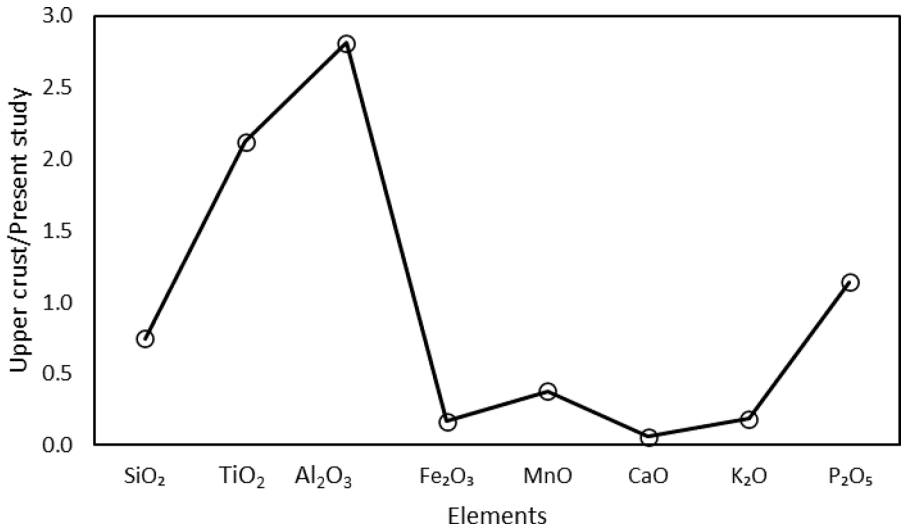

Fig. 3. Plot of upper crust elements mass fraction provided by Rudnick & Gao. (2003)[37] divided by the element's mass fraction obtained in the present study.

Results and discussion

Elemental composition of the investigated soil samples

The detailed description of the elemental composition of the samples can be found at[31]. The average mass fractions of major and minor elements in the ten soil samples under investigation are presented in Table 4 and illustrated in Fig. 4. SiO_2 (44.32–53.89%, with a mean value of 49.81%) and Al_2O_3 (39.79–46.32%, with a mean value of 42.18%) were the most abundant elements across all the soil samples. The remaining elements follow a specific order. The mean values of the components in descending order were as follows: Fe_2O_3 (0.001033-0.9560%, with a mean value of 0.856%), TiO_2 (1.183–1.607%, with a mean value of 1.360%), K_2O (0.2988–0.8478%, with a mean value of 0.5273%), CaO (0.0206–0.5666%, with a mean value of 0.2206%), P_2O_5 (0.0417–0.3503%, with a mean value of 0.1711%), MnO (0.0143–0.0715%, with a mean value of 0.0378%), and SO_3 (0.0000-0.0639%, with a mean value of 0.0106%). Na_2O and MgO were not detected, likely because they were present in very low mass fractions in the sample and are light elements on the periodic table, making them difficult to detect by EDXRF.

The low levels of TiO_2, K_2O, CaO, P_2O_5, and SO_3 in the soil samples investigated are attributed to the loss of these elements during alteration[32]. These elements are highly mobile in acidic soil[33,34]. Conversely, the high abundances of SiO_2, Al_2O_3, and Fe_2O_3 are due to the enrichment of these elements, which have low mobility. The soil geochemistry results indicate that the primary components are SiO_2, Al_2O_3, and Fe_2O_3, which is consistent with the elemental composition of other soil samples analyzed in various research studies[18,33,35,36]. SiO_2 and Al_2O_3 are nearly equal in magnitude ($SiO_2/Al_2O_3 = 1.18$). Of the samples analyzed, the highest and lowest levels of SiO_2 are found in samples M4 at 53.89% and M3 at 44.32%, respectively. The highest and lowest levels of Al_2O_3 are obtained from samples M3 (46.32%) and M4 (39.79%), respectively. The Fe_2O_3 mass fraction is lower than

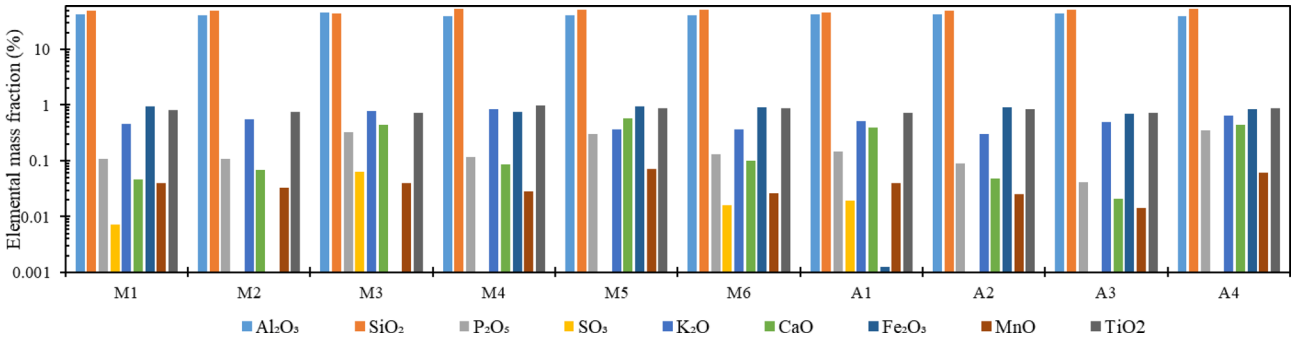

Fig. 4. Chart of the elemental mass fractions of major and minor elements in the investigated soil samples.

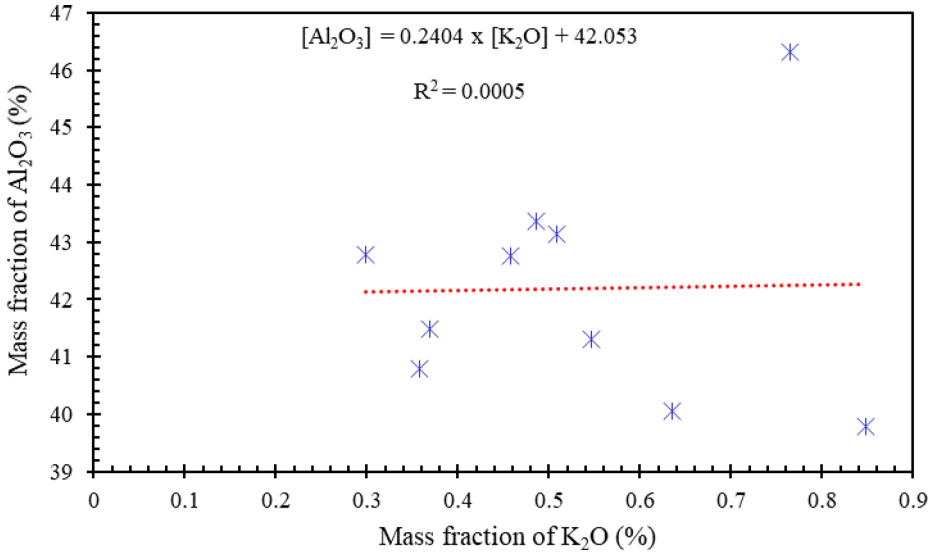

Fig. 5. A slightly positive correlation ($R^2 = 0.0005$) between K_2O and Al_2O_3 elemental mass fraction in the investigated soil samples.

that of SiO_2 and Al_2O_3, with the lowest value obtained for M3 (0.001033%) and the highest value obtained for M1 (0.9560%).

The comparison of major elements mass fractions obtained in the present work with the upper crust major elements mass fraction provided by Rudnick & Gao. (2003)[37] is illustrated in Fig. 3. The plot reveals substantial geochemical deviations. Notably, the elemental concentrations of Al_2O_3 and TiO_2 in the present study were 2.81 and 2.13 times higher than those provided by Rudnick & Gao (2003), respectively; whereas, the mass fractions of CaO, Fe_2O_3, K_2O, and MnO were about 16.24, 5.88, 5.31, and 2.63 times smaller than the upper crust values of Rudnick & Gao (2003)[37], respectively. These variations are characteristic of tropical weathering profiles, where intense leaching under humid conditions depletes base cations and enriches immobile elements such as Al or Ti.

The high Al_2O_3 content combined with the marked deficiency of nutrient-bearing oxides such as CaO, K_2O, and P_2O_5 confirms the feralitic nature of the soil in the study area, consistent with prior studies reported by Ben-Bolie et al. (2013)[9]. This could be explained by the fact that these soils are formed under sustained chemical weathering of aluminosilicate bedrock in the equatorial climate zone, leading to residual accumulation of aluminum oxides and iron oxides and loss of nutrient elements. Considering the fact that the study area lies within an agricultural zone adjacent to the uranium-bearing area of Lolodorf, the observed depletion in essential macronutrients such as potassium and calcium raises concern for long-term soil fertility and food crop productivity. Farmers relying on such soils may face challenges in maintaining yields without substantial amendments. Moreover, the natural geochemical background influenced by uranium mineralization may enhance the mobility and bioavailability of certain trace metal elements (TMEs), thereby posing potential risks to food safety and human health. These findings underscore the importance of integrating geochemical monitoring with agricultural land management and public health policies in uranium-bearing regions.

Geological provenance of the soil in the investigated area

The positive correlation between K_2O and Al_2O_3 presented in Fig. 5 indicates that the mass fraction of K-bearing minerals significantly affects the Al distribution. This suggests that clay minerals primarily control the relative

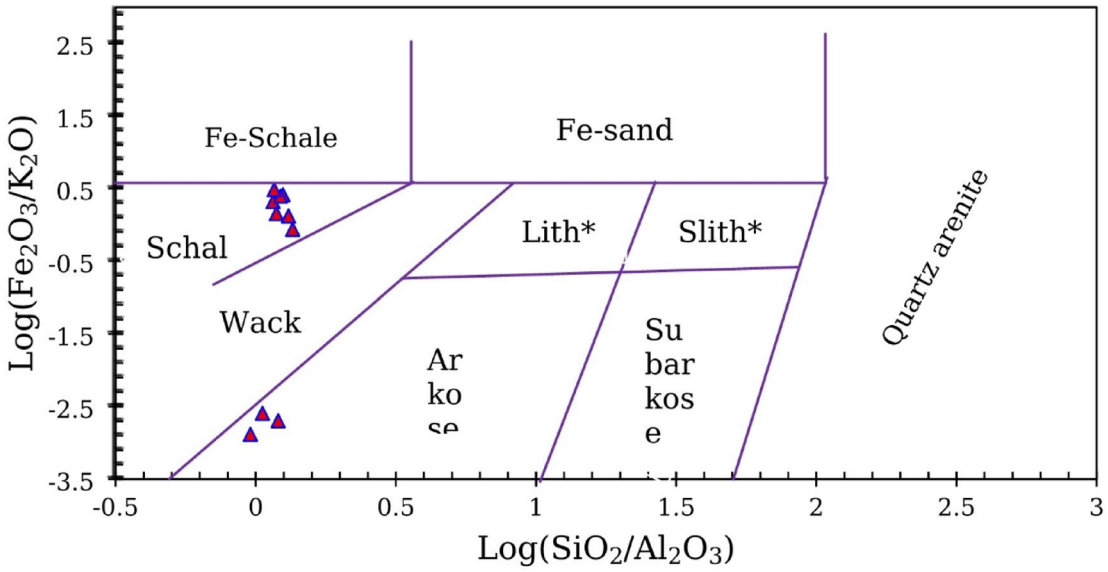

Fig. 6. Diagram of Chemical classification of analyzed soil samples based on discrimination diagrams using log (SiO_2/Al_2O_3) and log (Fe_2O_3/K_2O) values ([37]). *Lith refers to litharenite, and Slith refers to sublitharenite.

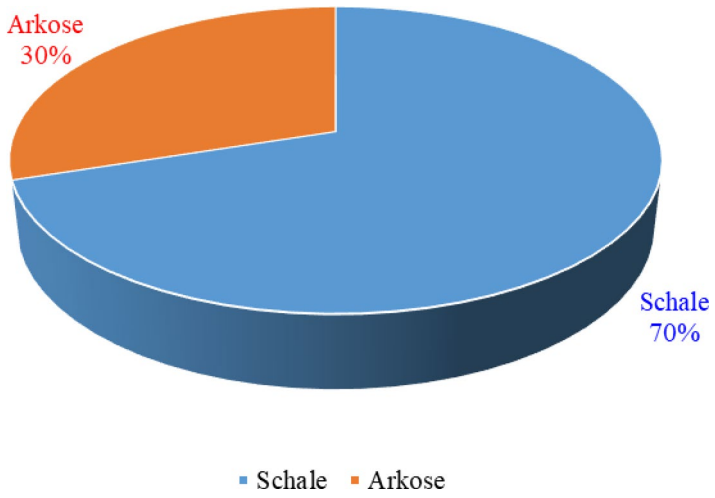

Fig. 7. Frequency diagram showing the classification of the investigated soil samples into two groups.

abundance of Al[33,38]. The diagrams presented in Figs. 6 and 7 depict Herron's classification[39] of the investigated soil samples into two distinct categories and the frequency distribution of the classification. Shale accounted for 70% (M1, M4, M5, M6, A2, A3, and A4), and arkose accounted for 30% (M2, M3, A1) of the samples collected from the investigated area within the Gulf of Guinea coast and its environs. These findings reflect the continuous weathering process in the area[23,40,41]. Weathering is the most active effect in place in the investigated area. The elemental mass fraction of soil rock is affected by pre-, syn-, and post-depositional conditions and processes that are to be considered for tectonic classification. These conditions and processes include the soil type available for erosion, the meteorological conditions or climate, the sorting effects, the biogenic material (carbonate, phosphate, and silica), and secondary minerals[22].

Figure 8 shows TiO_2 (%) as a function of Fe_2O_3+MgO (%). This diagram is compared with the well-known diagram for the tectonic discrimination of geological land or sediment provenance published by Bhatia[42]. As can be seen in Fig. 8, it is clear that all the investigated soil samples are representative of the residue from the passive margin. This finding is in line with the result published by Guembou et al. (2019) about sand samples collected from Douala, in the Littoral region of Cameroon, about 300 km away from the site investigated in the present study[19].

Figure 9 illustrates the proportion of Al_2O_3/SiO_2 (%) as a function of Fe_2O_3 + MgO (%). To understand the current processes in the research area, a tectonic discrimination diagram can be used to track the origin of the samples investigated to understand some processes that are continuing in the study area[42,43]. From the

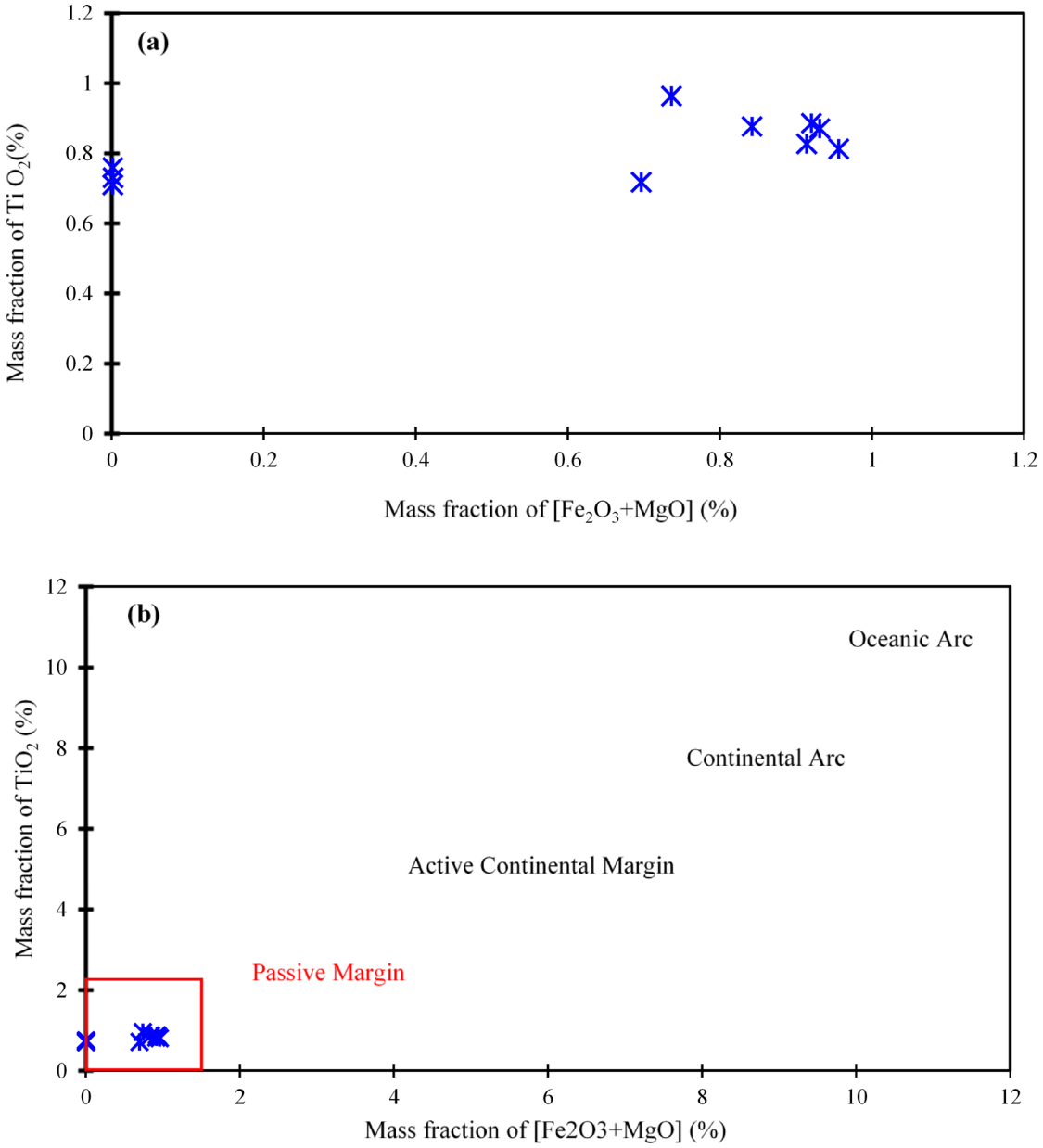

Fig. 8. TiO_2 (%) as a function of the Fe_2O_3 + MgO (%) diagram (a diagram for the tectonic discrimination of sediment provenance) plot for all investigated sample points: (**a**). Direct scale visualization; (**b**). The classification diagram indicates that the samples from the study area have passive margin provenances, with no samples having continental margin, continental arc, or oceanic arc provenances.

figures drawn here, it is evident from the comparison of the two diagrams that the investigated samples are all residual materials derived from passive margins. Similar conclusions were drawn in research studies published by Guembou et al. (2019)[19]. Compared to previous studies, the results obtained in this research support the data provided by previous authors. The investigated area is part or linked to the Gulf of Guinea characterized by low relief land and long river systems that extend from the shore land to the Atlantic Ocean, and a collection of thick piles of sedimentary detritus on the main shelves[44,45]. Therefore, weathering and erosion processes have a major effect on the geological provenance of the investigated areas. Moreover, the soil (geological materials) found in the Gulf of Guinea is acidic intrusive igneous resulting from the alteration of granite rock type and metamorphic as gneiss rock type. It also justifies the observed high levels of SiO_2 and Al_2O_3 found in the investigated samples[43,46].

The findings of this study suggest that the examined and surrounding regions were shaped by erosion and weathering processes rather than tectonic activity. The area mostly consists of acidic metamorphic rocks such as gneiss, syenite, and amphibolo-pyroxenite, and no evidence of tectonic activity has been found in the area. Previous research has confirmed that this location is situated within the Gulf of Guinea, a passive continental margin[18,36]. Using the elemental composition of soil samples to determine their geological origin is an active area of research, as demonstrated in this paper and in previous research[18–20,47]. In Cameroon, Schluter's (2008)

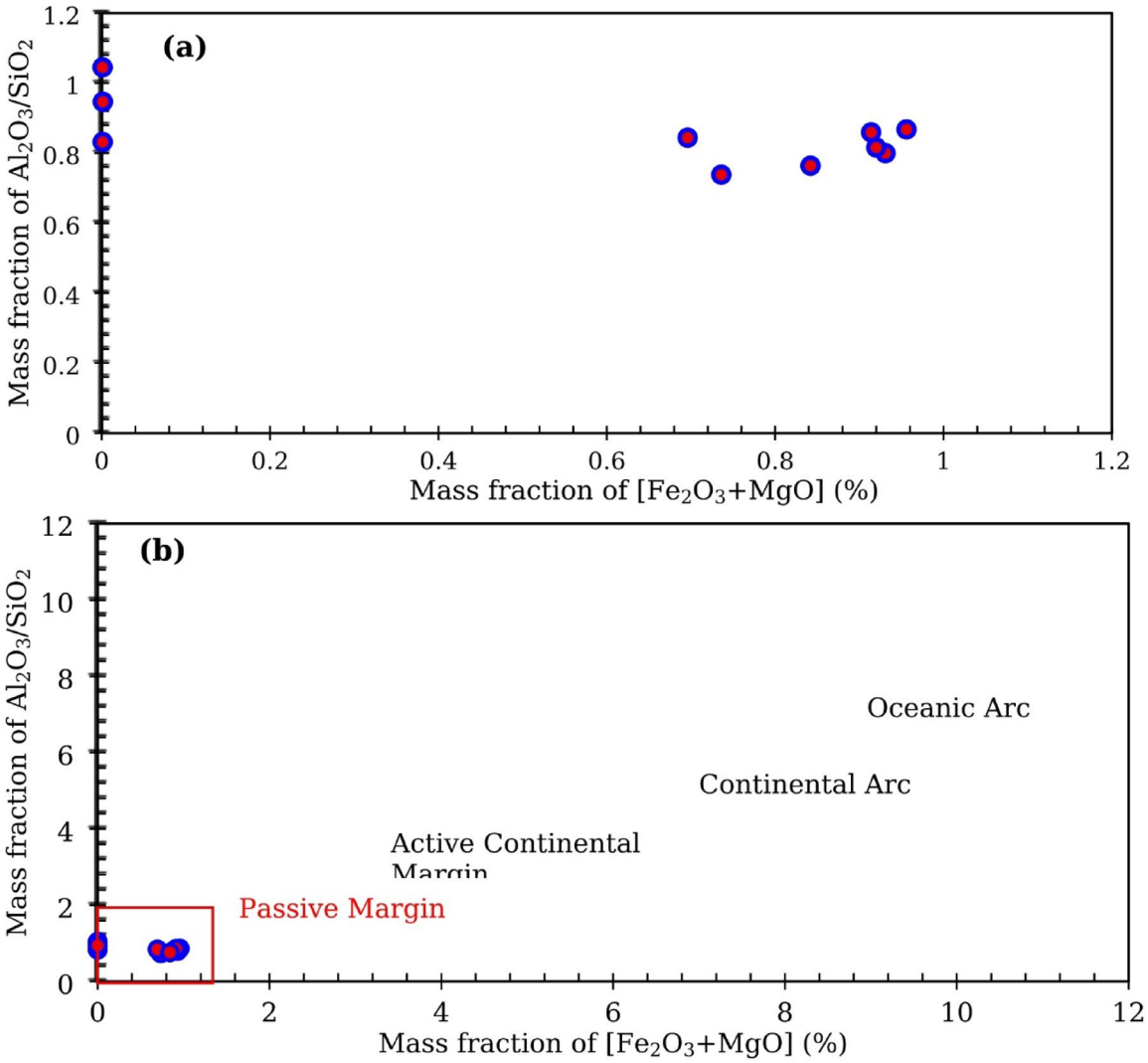

Fig. 9. AlO_3/SiO_2 (%) as a function of Fe_2O_3 + MgO (%): (**a**). Direct scale visualization; (**b**). A classification diagram showing that all the samples are from the passive margin.

research reveals that the Douala and Rio-del-Rey offshore basins are classic examples of passive margin basins that originated during the opening of the Atlantic Ocean. This finding sheds light on the geological history of these regions and highlights their potential for further exploration and study[19,48]. Therefore, the conclusions drawn in the present research are plausible evidence of the extension of the passive margin to the Mvengue and Awanda localities.

The enrichment in Al_2O_3 and TiO_2, along with the depletion of CaO, K_2O, and P_2O_5, supports a ferrallitic weathering profile typical of equatorial passive margins. These compositional patterns reflect prolonged chemical weathering and the influence of local parent rock, possibly of granitic and metasedimentary origin. Such mineralogical compositions are consistent with soils derived from the weathering of Precambrian basement rocks commonly observed in Southern Cameroon. Although this study does not focus on trace metal mobility, it is important to note that the dominance of Al and Fe oxides may influence the retention of trace elements, including those of potential environmental concern. In agricultural zones near uranium-bearing formations, such as the Mvengue Subdivision, these geochemical properties can play an indirect role in nutrient cycling and metal transport, meriting further investigation in future studies using the overall elemental composition obtained[31].

Conclusions

Quantitative analysis was carried out on soil samples collected from two localities, Mvengue and Awanda, located near the uranium deposit in South Cameroon, using an EDXRF Spectro Xepos spectrometer. The mass fractions of major oxide elements were utilized to determine the geochemistry of the area under investigation. Initially, the correlation between Al_2O_3 and K_2O was studied by plotting Al_2O_3 as a function of K_2O, which revealed a positive correlation. Next, chemical classification of the analyzed soil sample was carried out using Herron's discrimination diagram, revealing two types of sediments: shale and arkose. Finally, tectonic diagrams

illustrating the geological provenance of sediment and land were plotted. These diagrams demonstrate that the study area lies within the continental passive margin. The data obtained from this study are consistent with previous research, which showed that the study area is located in the Gulf of Guinea, a passive continental margin with no tectonic activity. The soil in this area is a product of weathering and erosion processes. The present findings help to elucidate the process of soil formation, and our future studies will focus on identifying the presence of uranium and petroleum resources in these localities. In addition, the data will serve as a baseline for the geochemistry of the area.

While the findings primarily inform the geological history of the study area, they also provide a foundational understanding of soil geochemistry relevant to evaluating trace element mobility and nutrient dynamics in surrounding agricultural environments. The results yielded by the present research can serve as an initial database for assessing the elemental composition of soils in the localities of Mvengue and Awanda and as a guide for future studies.

Data availability

The data and materials used to support the findings and conclusions of this manuscript are openly available and accessible to readers. Any data and materials not directly include in the manuscript will be made promptly available upon request from the corresponding author.

Received: 2 May 2025; Accepted: 26 August 2025
Published online: 15 October 2025

References

1. Taylor, S. R. & McLennan, S. M. *The Continental Crust: its Composition and Evolution. Reviews of Geophysics* (Blackwell Scientific Pub., 1985).
2. Cullers, R. L. The geochemistry of shales, siltstones and sandstones of Pennsylvanian–Permian age, colorado, USA: implications for provenance and metamorphic studies. *Lithos* **51**, 181–203 (2000).
3. Roser, B. P. & Korsch, R. J. Provenance signatures of sandstone-mudstone suites determined using discriminant function analysis of major-element data. *Chem. Geol.* **67**, 119–139 (1988).
4. Félix, B. A. J. et al. Determination of uranium in rocks and soils of South Cameroon by γ-ray spectrometry. *Radioisotopes* **60**, 399–408 (2011).
5. Abiama, P. E., Ateba, P. O., Ben-Bolie, G. H., Ekobena, F. H. P. & El Khoukhi, T. High background radiation investigated by gamma spectrometry of the soil in the Southwestern region of Cameroon. *J. Environ. Radioact.* **101**, 739–743 (2010).
6. Ateba, J. F. B. et al. Natural background dose measurements in South Cameroon. *Radiat. Prot. Dosimetry.* **140**, 81–88 (2010).
7. Mvondo, S., Ben-Bolie, G. H., Ema'a, J. M. E., Ateba, P. O. & Ateba, J. F. B. Study of soil-fern transfer of naturally occurring alpha emitting radionuclides in the Southern region of Cameroon. *J. Environ. Radioact.* **180**, 114–119 (2017).
8. Mvogo Aloa B., Beyala Ateba J. F., Guembou Shouop C. J., Ema'a Ema'a J. M., Sabouang J. F., Gondji D. S., & Ben-bolie G. H. (2025). Assessment of Trace Elements and their Health Impacts from Vegetable Consumption in the Vicinity of the Lolodorf Uranium Deposit, Southern Cameroon. Biological Trace Element Research. https://doi.org/10.1007/s12011-025-04760-5
9. Ben-Bolie, G. H., Abiama, E., Owono Ateba, P. & Khoukhi, P. E. Cherkaoui El moursli, R. Transfer of 238U and 232Th from soil to plant in a high background radiation area of the Southwestern region of Cameroon. *Radiat. Prot. Dosimetry.* **157**, 298–302 (2013).
10. Abiama, P. E. et al. Annual intakes of 226Ra, 228Ra and 40K in staple foodstuffs from a high background radiation area in the Southwest region of Cameroon. *J. Environ. Radioact.* **110**, 59–63 (2012).
11. Plant, J. A., Hale, M. & Ridgway, J. Developments in regional geochemistry for mineral exploration. *Appl. Earth Sci.* **97**, B116–B140 (1988).
12. Plant, J. A. & Hale, M. Handbook of exploration. *J. Geochemical.* **54**, 149–151 (1995).
13. Winefordner, J. D., Gornushkin, I. B., Correll, T., Gibb, E. & Smith, B. W. Comparing several atomic spectrometric methods to the super stars: special emphasis on laser induced breakdown spectrometry, LIBS, a future super star {. 1061–1083 (2004).
14. Banas, D., Braziewicz, J., Kubala-Kukus, A., Majewska, U. & Pajek, M. Study of absorption properties of chemically modified Halloysite samples with X-ray fluorescence and X-ray powder diffraction methods. *Radiat. Phys. Chem.* **93**, 129–134 (2013).
15. Fittschen, U. E. A. & Falkenberg, G. Trends in environmental science using microscopic X-ray fluorescence. *Spectrochim Acta Part. B Spectrosc.* **66**, 567–580 (2011).
16. Börjesson, J. & Mattsson, S. Medical applications of X-ray fluorescence for trace element research. *Powder Diffr.* **22**, 130–137 (2007).
17. Guembou, J. C. S. et al. Simultaneously gamma spectrometry & energy dispersive X-ray fluorescence-based color differentiation analysis of Douala-Bassa area's soil. *Environ. Technol. Innov.* **16**, 100486 (2019).
18. Guembou, J. C. S. et al. Elemental quantification and radioactive characterization of soil from Douala Bassa area: Littoral region of Cameroon using X-and γ-rays spectrometry. *Environ. Res. Commun.* **1**, 65001 (2019).
19. Guembou, J. C. S. et al. Determination of the natural radioactivity, elemental composition and geological provenance of sands from Douala in the Littoral region of Cameroon using X-ray and γ-ray spectrometry. *Appl. Earth Sci.* **128**, 167–180 (2019).
20. Guembou Shouop, C. J., Moyo, N., Nguelem Mekongtso, M., Motapon, E. J., Strivay, D. & O. & Application of energy dispersive X-ray fluorescence, γ-ray spectrometry and multivariate statistical approach for the classification of soil/sand from Douala-Cameroon. *Radiat. Phys. Chem.* **188**, 109589 (2021).
21. Shouop, C. J. G. et al. Recovering and restitution of unknown, unidentified, and unlabeled samples in laboratories using EDXRF analysis. *MethodsX* **8**, 101435 (2021).
22. Augustsson, C. et al. Provenance from the geochemical composition of terrestrial clastic deposits — A review with case study from the intracontinental Permo-Triassic of European Pangea. *Sediment. Geol.* **456**, 106496 (2023).
23. Shane, D., Charles, S., Thomas, M. H., Chen, S. & F, M. & Extremely high resolution XRF core scanning reveals the early triassic depositional history of the Montrey formation in Northeastern British columbia, Canada. *Palaeogeogr Palaeoclimatol Palaeoecol.* **637**, 112019 (2024).
24. Degbe, P. L. et al. Elemental characterization of quartzite of Pouma sub-division of Cameroon and radiation Attenuation properties based on XCOM and GEANT4 Monte Carlo simulation. *Radiat. Eff. Defects Solids.* **177**, 688–705 (2022).
25. Souffit, G. D., Mohamadou, L. L. & Shouop, G. Beyala ateba, J. F. Assessment of trace elements pollution and their potential health risks in the cobalt–nickel bearing areas of lomié, East Cameroon. *Environ. Monit. Assess.* **194**, 127 (2022).
26. Degbe, P. L. et al. Assessment of heavy metals' pollutions and potential risks associated to the rocks of Pouma subdivision-Cameroon. *Environ. Monit. Assess.* **195**, 1292 (2023).
27. Sighomnou, D. Analyse et redéfinition des régimes climatiques et hydrologiques du cameroun: perspectives d'évolution des ressources En eau. *These Doct Etat Univ. Yaoundé I Cameroun* (2004).

28. Markus, K., Jürgen, G., Christoph, B., Rudolf, B. & Franz, R. World map of the Köppen-Geiger climate classification updated. *Meteorol. Z.* **15**, 259–263 (2006).
29. Ottou, E. J. M. et al. Analyse morphotectonique par Couplage d'un modèle numérique de terrain (MNT) et des Données de terrain d'une portion de zone mobile paléoprotérozoïque de La région de Lolodorf (Complexe du nyong, SW Cameroun). *Sci. Technol. Développement*. **15**, 9–25 (2014).
30. Abdourahimi, S., Fantong, W. Y., Aka, F. T. & Njock, M. G. K. Environmental pollution by metals in the oil bearing Bakassi peninsula, Cameroon. *Carpathian J. Earth Environ. Sci.* **11**, 529–538 (2016).
31. Mvogo Aloa, B. et al. Assessment of contamination levels, potential ecological and human health risks due to trace elements pollution in the vicinity of the Lolodorf uranium deposit, Southern Cameroon. *Environ. Monit. Assess.* **196**, 1147 (2024).
32. Rajendrakumar, B. & Ganapathi, P. Redistribution and mass change geochemistry during weathering of laterites from the Swarnagadde plateau, Uttar Kannada district, karnataka, India. *Indian J. Appl. Res.* **8**, 53–56 (2018).
33. Caridi, F., Messina, M. & D'agostino, M. An investigation about natural radioactivity, hydrochemistry, and metal pollution in groundwater from Calabrian selected areas, Southern Italy. *Environ. Earth Sci.* **76**, 668 (2017).
34. Clemente, R., Dickinson, N. M. & Lepp, N. W. Mobility of metals and metalloids in a multi-element contaminated soil 20 years after cessation of the pollution source activity. *Environ. Pollut.* **155**, 254–261 (2008).
35. Tchameni, R., Mezger, K., Nsifa, N. E. & Pouclet, A. Crustal origin of early proterozoic syenites in the congo craton (Ntem complex), South Cameroon. *Lithos* **57**, 23–42 (2001).
36. Anani, C. Y., Mahamuda, A., Kwayisi, D. & Asiedu, D. K. Provenance of sandstones from the neoproterozoic Bombouaka group of the Volta basin, Northeastern Ghana. *Arab. J. Geosci.* **10**, 1–15 (2017).
37. Rudnick, R. L. & Gao, S. Composition of the continental crust. *Treatise Geochem. 2nd Ed.* **3**, 1–64 (2003).
38. McLennan, S. M., Taylor, S. R. & Eriksson, K. A. Geochemistry of archean shales from the Pilbara supergroup, Western Australia. *Geochim. Cosmochim. Acta*. **47**, 1211–1222 (1983).
39. Herron, M. M. Geochemical classification of terrigenous sands and shales from core or log data. *J. Sediment. Res.* **58**, 820–829 (1988).
40. Lundblad, S. P., Mills, P. R. & Hon, K. Analysing archaeological basalt using non-destructive energy-dispersive X-ray fluorescence (EDXRF): effects of post-depositional chemical weathering and sample size on analytical precision. *Archaeometry* **50**, 1–11 (2008).
41. MAHSHAR, R. et al. Provenance and weathering history of Archaean Naharmagra quartzite of Aravalli craton, NW Indian shield : petrographic and geochemical evidence. *Geochem. J.* **44**, 331–345 (2010).
42. Bhatia, M. R. Plate tectonics and geochemical composition of sandstones. *J. Geol.* **91**, 611–627 (1983).
43. Bhatia, M. R. Rare Earth element geochemistry of Australian paleozoic graywackes and mudrocks: provenance and tectonic control. *Sediment. Geol.* **45**, 97–113 (1985).
44. Tchouankoue, J. P. & Petrology Geochemistry, and geodynamic implications of basaltic Dyke swarms from the Southern continental part of the Cameroon volcanic line, central Africa. *Open. Geol. J.* **6**, 72–84 (2012).
45. MARZOLI, A. et al. The Cameroon volcanic line revisited: petrogenesis of continental basaltic magmas from lithospheric and asthenospheric mantle sources. *J. Petrol.* **41**, 87–109 (2000).
46. Déruelle, B., Ngounouno, I. & Demaiffe, D. The 'cameroon hot line' (CHL): A unique example of active alkaline intraplate structure in both oceanic and continental lithospheres. *Comptes Rendus Géoscience*. **339**, 589–600 (2007).
47. Hazou, E. et al. Heavy metal pollution assessment using energy-dispersive x-ray fluorescence and multivariate statistical approach of soil from phosphate ore sites, Southern region of Togo. *Water Air Soil. Pollut.* **232**, 489 (2021).
48. Thomas, S. *Geological Atlas of Africa* (Springer Berlin Heidelberg, Berlin, 2008). https://doi.org/10.1007/978-3-540-76373-4

Acknowledgements

The authors would like to extend their thanks to the Cameroon Radiological Safety and Nuclear Security Authority for the technical support and equipment provided during EDXRF spectra acquisition and data analysis and most especially for their useful discussions, guidance, and help provided in reviewing the manuscript and for making their facilities available for this research work. We would like to thank the Research Centre for Nuclear Science and Technology, Institute of Geological and Mining Research (IRGM), Cameroon, for the technical support and equipment provided during sample preparation. We would also like to thank the local communities of Mvengue and Awanda during the sampling campaign for their guidance in the field.

Author contributions

Field work and samples preparation have been conducted by Bonaventure MVOGO ALOA under the supervision of Jean Félix BEYALA ATEBA and Germain Hubert BEN-BOLIE. Measurements have been conducted within the National Radiation Protection Agency laboratory by Jean Faustin SABOUANG and Cébastien GUEMBOU SHOUOP assisted by Bonaventure MVOGO ALOA under the supervision of Jean Félix BEYALA ATEBA. Data analysis was performed by Jean Marie EMA'A EMA'A, Bonaventure MVOGO ALOA and Dieu Soffit GONDJI under the supervision of Jean Félix BEYALA ATEBA and Germain Hubert BEN-BOLIE. Manuscript has been drafted by Bonaventure MVOGO ALOA and revised by each co-author. Figures have been done by Cébastien GUEMBOU SHOUOP and Bonaventure MVOGO ALOA under the supervision of Jean Félix BEYALA ATEBA and Germain Hubert BEN-BOLIE.

Funding

The authors declare that no funds, grants, or other support were received during the preparation of this manuscript.

Declarations

Competing interests

The authors declare no competing interests.

Additional information

Correspondence and requests for materials should be addressed to J.F.B.A.